electronics

MDPI

Article

Adaptive Discontinuous Control for Fixed-Time Consensus of Nonlinear Multi-Agent Systems

Lu Wang [1], Min Zou [1], Wanli Guo [1,*], Hajid Alsubaie [2], Ahmed Alotaibi [2], Rasha Osman Ahmed Taie [3] and Hadi Jahanshahi [4,*]

[1] School of Mathematics and Physics, China University of Geosciences, Wuhan 430074, China
[2] Department of Mechanical Engineering, College of Engineering, Taif University, Taif 21944, Saudi Arabia
[3] Department of Mathematics, Faculty of Science, Assiut University, Assiut 71516, Egypt
[4] Department of Mechanical Engineering, University of Manitoba, Winnipeg, MB R3T 5V6, Canada
* Correspondence: guowanliff@163.com (W.G.); jahanshahi.hadi90@gmail.com (H.J.)

Abstract: This paper mainly focuses on the fixed-time consensus (FXC) control problem for nonlinear multi-agent systems (MASs). For the cases of leader-following and leaderless, two adaptive discontinuous protocols are designed, respectively, to realize our control goals. Common adaptive control protocols always significantly increase the dimension of the considered system model, while the protocols presented here only require two adaptive update laws and are therefore simpler to apply in the engineering control. Moreover, no additional conditions are required to ensure that the system can achieve FXC successfully, except for some necessary assumptions. Simulation examples also illustrate that these two protocols are effective.

Keywords: leader-following multi-agent systems; leaderless multi-agent systems; fixed-time consensus; adaptive discontinuous protocol

check for updates

Citation: Wang, L.; Zou, M.; Guo, W.; Alsubaie, H.; Alotaibi, A.; Osman Ahmed Taie, R.; Jahanshahi, H. Adaptive Discontinuous Control for Fixed-Time Consensus of Nonlinear Multi-Agent Systems. *Electronics* **2022**, *11*, 3545. https://doi.org/10.3390/electronics11213545

Academic Editors: Mahmut Reyhanoglu, Erkan Kayacan and Mohammad Jafari

Received: 5 October 2022
Accepted: 26 October 2022
Published: 30 October 2022

Publisher's Note: MDPI stays neutral with regard to jurisdictional claims in published maps and institutional affiliations.

Copyright: © 2022 by the authors. Licensee MDPI, Basel, Switzerland. This article is an open access article distributed under the terms and conditions of the Creative Commons Attribution (CC BY) license (https://creativecommons.org/licenses/by/4.0/).

1. Introduction

MAS is important content in the field of artificial intelligence. It is an interdisciplinary subject belonging to many fields such as computer, military, communication and control [1,2]. MAS has become an effective method and tool for analyzing, designing and modeling complex systems in reality. Through the introduction of multi-agent cooperation mechanism, a large-scale complex task can be completed by multiple simple agents, which can save the cost and reduce the waste of resources to a greater extent compared with highly intelligent agents. The consensus problem of MASs aims at guiding the states of agents towards a common value by using local interactions. It is the key to studying the cooperative and coordinated control of MAS. The formation problem of unmanned aerial vehicle [3,4], the management of supply chain networks [5,6], the cooperation of social networks [7], synchronization of smart power grid architectures [8], etc., are all based on the consensus of MASs.

After decades of research, a variety of consensus forms have been derived, such as asymptotic consensus [9,10], finite-time consensus [11–16] and FXC. Compared with the other two forms, FXC not only has a fast convergence rate, but also has a settling time that can be estimated by a uniform upper bound independent of the initial value of the system. Therefore, the FXC of MASs has attracted much attention from many scholars. At first, the focus was on linear MASs. For example, a time-based generator approach was proposed in [17] to investigate both leaderless and leader-following practical FXC for integrator-type linear MASs. In [18], Artstein–Kwon–Pearson reduction approach was utilized to study the event-triggered FXC for linear MASs with input delay. By means of the input shaping technique, Chen and Shan [19] designed a novel simple fixed-time protocol for the linear double-integrator MASs. Sliding mode protocol based on distributed

observers was presented in [20] to solve the FXC tracking control for the second-order MASs under directed communication topology.

However, most coupled dynamical systems in nature, physics, economy, and society are nonlinear. Because of this, nonlinear MASs should be the main research object. Based on event-triggered strategies, FXC protocols were presented for both the centralized and the distributed consensus of nonlinear MASs in [21]. In [22], the authors considered the FXC problem for nonlinear MASs with general time-varying topologies and stochastically switching topologies via appropriate nonlinear control protocols. Some discontinuous control protocols were developed in [23] to investigate the fixed-time bipartite consensus issue for nonlinear disturbed MASs. By means of an observer-based decentralized controller, ref. [24] addressed the FXC tracking problem for nonlinear second-order MASs under directed topology.

Generally speaking, a FXC control protocol for nonlinear MASs often contains multiple power state feedbacks. Although this control strategy could drive the system to the ultimate goal, the control tradeoff and cost may be bound to be high. As an economical and effective control method, adaptive protocols are widely exploited in the consensus control of MASs. This is because the structure of the adaptive control method can be adjusted in real time according to the current operating state of the system. Actually, owing to the superiority, many adaptive control protocols have been employed in FXC of MASs [25–31]. In [25], distributed node-based adaptive control protocols were used to study the fixed-time leader-following and containment consensus for MASs. By presenting distributed observers, ref. [26] studied the adaptive FXC tracking problem for uncertain MASs with output constraints. In [27], the FXC tracking for the MASs with discontinuous dynamics was solved, in which all the control gains adopt an adaptive strategy. By employing fixed-time control and neural networks, an adaptive fixed-time control approach was developed in [28]. A novel adaptive fixed-time controller was designed in [29,30] by combining the Lyapunov stability theory. In [31], an adaptive controller was designed to ensure the FXC by introducing fuzzy logic system and a backstepping technique. It must be pointed out that the adaptive protocols used above significantly increase the dimension of the system model. Each agent or each edge of the system was assigned to at least one adaptive update law. Therefore, the design of these control protocols will increase the complexity of theoretical analysis and numerical simulation, and will also bring more restrictions to engineering applications. Can a class of simple control protocol based on fewer adaptive update laws be designed to achieve FXC of MASs? This is a problem worth pondering and challenging.

Inspired by above discussions, this paper aims to design simple adaptive control protocols to study the FXC problems for nonlinear leader-following and leaderless MASs, respectively. The main contributions are stated as follows. Two novel adaptive FXC control protocols for nonlinear leader-following and leaderless MASs are proposed, respectively. These two control protocols only require the state measurement errors and their sign information, which is simpler in structure than the control protocol proposed in [25,27–37]. Compared with the common adaptive control methods [25–27], these two protocols presented here only need two adaptive update laws, regardless of the scale of the system. Furthermore, no additional conditions are required to guarantee the FXC of the system, except for some necessary assumptions. Lastly, the chaotic multi-agent supply chain networks are used as simulation examples to verify the effectiveness of the proposed control protocols.

Notations: R^m, $||\cdot||_m$ and $R^{m\times m}$ denote m-dimensional real vector space, the Euclidean m-norm, and $m \times m$ real matrix space, respectively; $\mathrm{diag}(\xi_1, \xi_2, \ldots, \xi_m)$ is a diagonal matrix whose diagonal elements are $\xi_1, \xi_2, \ldots, \xi_m$; 1_m represents the column vector $(1, 1, \ldots, 1)_m^T$. For $z = (z_1, z_2, \ldots, z_m)^T$, we give the following notations: the power of the vector z is defined as $z^\delta = (z_1^\delta, z_2^\delta, \ldots, z_m^\delta)^T$, where $\delta \in R$; $\mathrm{sign}(z) = (\mathrm{sign}(z_1), \mathrm{sign}(z_2), \ldots, \mathrm{sign}(z_m))^T$, where $\mathrm{sign}(\cdot)$ is the signum function; $\mathrm{sig}^\delta(z) = (\mathrm{sig}^\delta(z_1), \mathrm{sig}^\delta(z_2), \ldots, \mathrm{sig}^\delta(z_m))^T$, where $\mathrm{sig}^\delta(z_i) = |z_i|^\delta \mathrm{sign}(z_i)$; $\mathbb{S}\mathrm{ign}(z) = (\mathbb{S}\mathrm{ign}(z_1), \mathbb{S}\mathrm{ign}(z_2), \ldots, \mathbb{S}\mathrm{ign}(z_m))^T$, where $\mathbb{S}\mathrm{ign}(\cdot)$ is

a set-valued function defined as: when $\varsigma \neq 0, \mathbb{S}\text{ign}(\varsigma) = \text{sign}(\varsigma)$, and when $\varsigma = 0$, $\mathbb{S}\text{ign}(\varsigma) = [-1, 1]$.

2. Useful Preliminaries

Graph Theory

Graph $G_A = (\mathcal{V}, \Im, A)$ is used to indicate the topology of information communication among agents in a MAS. In the graph G_A, $\mathcal{V} = \{v_1, v_2, \ldots, v_n\}$ is the set of all agents in the system, $\Im$ is the edge set representing the connection between agents, and $A = (a_{ij})_{n\times n}$ is the weighted adjacency matrix describing the intensity of information communication. The element a_{ij} of matrix A is positive if and only if $(v_i, v_j) \in \Im$; otherwise, $a_{ij} = 0$. This paper does not consider self-loop, which implies $a_{ii} = 0$. A sequence of edges $(v_i, v_i^1), (v_i^1, v_i^2), \ldots, (v_i^k, v_j)$ with distinct agents $v_i^1, v_i^2, \ldots, v_i^k$ is called a path from agent v_i to v_j. Graph G_A is said to contain a spanning tree if there is at least one agent (named root) with the property that one or more paths exist from it to any other agent.

Definition 1. *If at least one path exists between any two agents, then G_A is called strongly connected.*

Definition 2 ([14])**.** *If positive constants $q_1, q_2, \ldots, q_n$ exist, such that $q_i a_{ij} = q_j a_{ji}$, for $i, j = 1, 2, \ldots, n$, then the directed graph G_A is detail balanced.*

We define the Laplacian matrix $L_A = \text{diag}(\sum_{j=1}^{n} a_{1j}, \sum_{j=1}^{n} a_{2j}, \ldots, \sum_{j=1}^{n} a_{nj}) - A$. If G_A is detail balanced with positive constants $q_1, q_2, \ldots, q_n$, then it is not difficult to find that QL_A is symmetric with $Q = \text{diag}(q_1, q_2, \ldots, q_n)$. In fact, QL_A is equivalent to the Laplacian matrix of an undirected graph which contains the same set of agents and the same set of edges, but a different weighted adjacency matrix from graph G_A.

Lemma 1 ([38])**.** *If graph G_A is strongly connected, then its Laplacian matrix has an eigenvalue of zero with multiplicity of one, and the remaining eigenvalues are positive. If graph G_A is also undirected, we have*

(1) $x^T L_A^2 x \geq \lambda_2(L_A) x^T L_A x$;

(2) $x^T L_A x \geq \lambda_2(L_A) x^T x$, and x satisfies $1_n^T x = 0$;

where $\lambda_2(L_A)$ is the second-smallest eigenvalue of L_A.

Lemma 2. *Suppose function $V(t)$ is positive definite. If $V(t)$ satisfies*

$$\dot{V}(t) \leq -bV^{\delta}(t) - cV^{\theta}(t),$$

where $0 < \delta < 1 < \theta$ and $b, c > 0$, then $V(t) \to 0$ in a fixed time, and the settling time T is estimated by

$$T \leq \frac{1}{b(1-\delta)} + \frac{1}{c(\theta-1)}.$$

Lemma 3 ([39])**.** *For any non-negative real numbers $z_1, z_2, \ldots, z_m$, the following inequalities hold:*

(1) $\sum_{k=1}^{m} z_k^h \geq (\sum_{k=1}^{m} z_k)^h$, when $0 < h \leq 1$;

(2) $\sum_{k=1}^{m} z_k^h \geq m^{1-h} (\sum_{k=1}^{m} z_k)^h$, when $h \geq 1$.

Lemma 4 ([39])**.** *For any vector $z = (z_1, z_2, \ldots, z_m)^T \in R^m$, $h_1 > h_2 > 0$, the following inequality holds*

$$(\sum_{k=1}^{m} |z_k|^{h_1})^{\frac{1}{h_1}} \leq (\sum_{k=1}^{m} |z_k|^{h_2})^{\frac{1}{h_2}} \leq m^{\frac{1}{h_2} - \frac{1}{h_1}} (\sum_{k=1}^{m} |z_k|^{h_1})^{\frac{1}{h_1}}.$$

3. Fixed-Time Leader-Following Consensus

In this section, we will study a MAS consisting of a leader (labeled 0) and n followers. The topology of a leader-following MAS is different from G_A, which not only contains the graph G_A, but also the edges between the leader and its followers. Denote $A_0 = \text{diag}(a_{10}, a_{20}, \ldots, a_{n0})$ as the leader adjacency matrix, if $a_{i0} > 0$, that is, an edge exists from the leader to the ith follower which means the follower can get information from the leader; otherwise, $a_{i0} = 0$.

Lemma 5 ([38]). *If graph G_A is undirected and the leader is the root of graph $\bar{G}_A$, then $L_A + A_0$ is positive definite.*

From the lemma above, it can be seen that if directed graph G_A is detail balanced and the root of $\bar{G}_A$ is the leader, then $QL_A + A_0$ is positive definite, where $Q = \text{diag}(q_1, q_2, \ldots, q_n)$.

Suppose that the considered leader-following MASs have the following dynamics

$$\begin{cases} \dot{x}_0(t) = f(x_0(t)), \\ \dot{x}_i(t) = f(x_i(t)) + u_i(t) + d_i(t), \ \ i = 1, 2, \ldots, n, \end{cases} \tag{1}$$

where $x_0(t), x_i(t) \in R^m$ are the leader's and the ith follower's state, respectively, nonlinear R^m valued vector function $f(x_i(t))$ reveals the dynamic properties of one isolated agent, and $u_i(t) \in R^m$ denotes the ith follower's control input to be designed, $d_i(t)$ is the bounded disturbance, i.e., $||d_i(t)|| \leq d$, and d is a positive constant.

Definition 3. *For the above leader-following system (1), if a positive constant T(named settling time) exists, such that*

$$\begin{cases} \lim\limits_{t \to T}(x_i(t) - x_0(t)) = 0, \\ x_i(t) = x_0(t), \forall t \geq T, \end{cases}$$

then the finite-time consensus tracking is achieved. Particularly, if T is independent of the initial values, we say that the FXC tracking of system (1) is achieved.

Assumption 1 ([40]). *For the nonlinear function $f(x)$ in system (1), a positive constant ρ exists, such that*

$$(x - y)^T (f(x) - f(y)) \leq \rho (x - y)^T (x - y), \ \forall x, y \in R^m.$$

Remark 1. *Lipschitz continuity is often used as a prerequisite for the existence and uniqueness of solutions to nonlinear ordinary differential equations. Many practical scenarios, including chaos and oscillation, are Lipschitz continuous. However, this assumption limits the local variation of the function $f(\cdot)$ to no greater than the increment of a linear function. This makes it impossible for many common functions, such as exponential and nonlinear polynomial functions, to satisfy this assumption. Recently, another upper bound structure for nonlinear dynamics and interconnections was presented in [41]. Based on this kind of assumption, the authors studied the synchronization problem for complex networks composed of nonlinear nodes under state-dependent a priori interconnections.*

In order to make system (1) achieve FXC, we design an adaptive discontinuous control protocol for the ith follower as

$$\begin{cases} u_i(t) = c_1(t) \text{sig}^{\alpha} \varphi_i(t) + (c_2(t) + d) \text{sign} \varphi_i(t), \\ \dot{c_1}(t) = \sum\limits_{i=1}^{n} \varphi_i(t) \text{sig}^{\alpha} \varphi_i(t), \\ \dot{c_2}(t) = \sum\limits_{i=1}^{n} \varphi_i(t) \text{sign} \varphi_i(t), \end{cases} \tag{2}$$

where $c_1(t), c_2(t)$ are adaptive control gains with $c_1(0), c_2(0) > 0$, power parameter $\alpha > 1$, and $\varphi_i(t) = \sum\limits_{j=1}^{n} q_i a_{ij}(x_j(t) - x_i(t)) + a_{i0}(x_0(t) - x_i(t))$.

After recording the state error as $e_i(t) = x_i(t) - x_0(t)$, we have the state error system as

$$\begin{cases} \dot{e}_i(t) = & f(x_i(t)) - f(x_0(t)) + c_1(t)\text{sig}^{\alpha}(\sum_{j=1}^{n} q_i a_{ij}(e_j(t) - e_i(t)) - a_{i0}e_i(t)) \\ & +(c_2(t)+d)\text{sign}(\sum_{j=1}^{n} q_i a_{ij}(e_j(t) - e_i(t)) - a_{i0}e_i(t)) + d_i(t), \\ \dot{c}_1(t) = & \sum_{i=1}^{n}(\sum_{j=1}^{n} q_i a_{ij}(e_j(t) - e_i(t)) - a_{i0}e_i(t))\text{sig}^{\alpha}(\sum_{j=1}^{n} q_i a_{ij}(e_j(t) - e_i(t)) - a_{i0}e_i(t)), \\ \dot{c}_2(t) = & \sum_{i=1}^{n}(\sum_{j=1}^{n} q_i a_{ij}(e_j(t) - e_i(t)) - a_{i0}e_i(t))\text{sign}(\sum_{j=1}^{n} q_i a_{ij}(e_j(t) - e_i(t)) - a_{i0}e_i(t)). \end{cases} \tag{3}$$

Thus, in the section, we will consider the fixed-time stability of the error system (3) instead of the FXC tracking problem of system (1).

In the following contents of this section, for the convenience of writing, we shall consider the simplest form; that is, $m = 1$, and the other cases shall be naturally generalized by the Kronecker product. At the same time, the time t in various time-related symbols will be omitted; for example, x_i will replace the state vector $x_i(t)$ of the ith agent.

Denote $e = (e_1, e_2, \ldots, e_n)^T$, $F(e) = (f(x_1) - f(x_0), f(x_2) - f(x_0), \ldots, f(x_n) - f(x_0))^T$, $D(t) = (d_1, d_2, \ldots, d_n)^T$. Then, the error system (3) can be written as its compact form

$$\begin{cases} \dot{e} = F(e) - c_1(t)\text{sig}^{\alpha}(\hat{L}e) - (c_2(t)+d)\text{sign}(\hat{L}e) + D(t), \\ \dot{c}_1(t) = \|\hat{L}e\|_{\alpha+1}^{\alpha+1}, \\ \dot{c}_2(t) = \|\hat{L}e\|_1, \end{cases} \tag{4}$$

where $\hat{L} = QL_A + A_0$.

Theorem 1. *Supposed that Assumption 1 holds, G_A is detail balanced, and the leader is the root of $\bar{G}_A$. Then, system (1) will achieve FXC tracking under the given protocol (2).*

Proof. Choose the following positive definite function

$$V = V_1 + V_2,$$

where $V_1 = \frac{1}{2}e^T\hat{L}e$, $V_2 = \frac{(c_1(t)-c_1^*)^2}{2} + \frac{(c_2(t)-c_1^*)^2}{2}$ with a big enough positive constant c_1^*.

The existence of the sign information of the state error in our control protocol (2) causes the discontinuity of the right hand of the concerned system (1), which results in its solution being of the Filippov sense [42]. So, we have the derivative of V with respect to time t as

$$\begin{aligned} \dot{V} =& \dot{V}_1 + \dot{V}_2 \\ \in& K[e^T\hat{L}\dot{e} + (c_1(t) - c_1^*)\dot{c}_1(t) + (c_2(t) - c_1^*)\dot{c}_2(t)] \\ =& e^T\hat{L}(F(e) - c_1(t)\text{sig}^{\alpha}(\hat{L}e) - (c_2(t)+d)\mathbb{S}\text{ign}(\hat{L}e) + D(t)) \\ & + (c_1(t) - c_1^*)||\hat{L}e||_{\alpha+1}^{\alpha+1} + (c_2(t) - c_1^*)||\hat{L}e||_1. \end{aligned}$$

According to the measurable selection theorem [42], there must be a measurable function $S(t) \in \mathbb{S}\text{ign}(\hat{L}e)$ that makes the following statement true.

$$\begin{aligned} \dot{V} =& e^T\hat{L}(F(e) - c_1(t)\text{sig}^{\alpha}(\hat{L}e) - (c_2(t)+d)S(t) + D(t)) \\ & + (c_1(t) - c_1^*)||\hat{L}e||_{\alpha+1}^{\alpha+1} + (c_2(t) - c_1^*)||\hat{L}e||_1 \\ =& e^T\hat{L}F(e) - c_1^*||\hat{L}e||_{\alpha+1}^{\alpha+1} - c_1^*||\hat{L}e||_1 - de^T\hat{L} + e^T\hat{L}D(t) \\ \le& \frac{1}{2}e^T\hat{L}e + \frac{1}{2}F(e)^T\hat{L}F(e) - c_1^* n^{\frac{1-\alpha}{2}}(||\hat{L}e||_2^2)^{\frac{\alpha+1}{2}} - c_1^*(||\hat{L}e||_2^2)^{\frac{1}{2}} \\ \le& \frac{1}{2}(1+\rho^2)e^T\hat{L}e - c_1^* n^{\frac{1-\alpha}{2}}(\underline{\lambda}e^T\hat{L}e)^{\frac{\alpha+1}{2}} - c_1^*(\underline{\lambda}e^T\hat{L}e)^{\frac{1}{2}} \\ \le& (1+\rho^2)V_1 - c_1^* 2^{\frac{\alpha+1}{2}} n^{\frac{1-\alpha}{2}}\underline{\lambda}^{\frac{\alpha+1}{2}}V_1^{\frac{\alpha+1}{2}} - 2^{\frac{1}{2}}c_1^*\underline{\lambda}^{\frac{1}{2}}V_1^{\frac{1}{2}}. \end{aligned}$$

Obviously, if c_1^* is big enough, it follows that

$$\dot{V} \leq 0,$$

which implies V, $c_1(t)$ and $c_2(t)$ are all bounded.

From Assumption 1, and noting the inequalities in Lemmas 3 and 4, we can obtain

$$\begin{aligned}
\dot{V}_1 =& \dot{V} - \dot{V}_2 \\
=& e^T\hat{L}F(e) - c_1^*||\hat{L}e||_{\alpha+1}^{\alpha+1} - c_1^*||\hat{L}e||_1 - de^T\hat{L} + e^T\hat{L}D(t) - (c_1(t) - c_1^*)||\hat{L}e||_{\alpha+1}^{\alpha+1} \\
& - (c_2(t) - {c_1}^*)||\hat{L}e||_1 \\
=& e^T\hat{L}F(e) - c_1(t)||\hat{L}e||_{\alpha+1}^{\alpha+1} - c_2(t)||\hat{L}e||_1 - de^T\hat{L} + e^T\hat{L}D(t) \\
\leq& e^T\hat{L}F(e) - c_1(0)||\hat{L}e||_{\alpha+1}^{\alpha+1} - c_2(0)||\hat{L}e||_1 \\
\leq& \frac{1}{2}e^T\hat{L}e + \frac{1}{2}F(e)^T\hat{L}F(e) - c_1(0)n^{\frac{1-\alpha}{2}}(||\hat{L}e||_2^2)^{\frac{\alpha+1}{2}} - c_2(0)(||\hat{L}e||_2^2)^{\frac{1}{2}} \\
\leq& \frac{1}{2}(1+\rho^2)e^T\hat{L}e - c_1(0)n^{\frac{1-\alpha}{2}}(\underline{\lambda}e^T\hat{L}e)^{\frac{\alpha+1}{2}} - c_2(0)(\underline{\lambda}e^T\hat{L}e)^{\frac{1}{2}} \\
\leq& (1+\rho^2)V_1 - c_1(0)2^{\frac{\alpha+1}{2}}n^{\frac{1-\alpha}{2}}(\underline{\lambda}V_1)^{\frac{\alpha+1}{2}} - 2^{\frac{1}{2}}c_2(0)(\underline{\lambda}V_1)^{\frac{1}{2}} \\
=& (1+\rho^2)V_1 - c_1(0)2^{\frac{\alpha+1}{2}}n^{\frac{1-\alpha}{2}}\underline{\lambda}^{\frac{\alpha+1}{2}}V_1^{\frac{\alpha+1}{2}} - 2^{\frac{1}{2}}c_2(0)\underline{\lambda}^{\frac{1}{2}}V_1^{\frac{1}{2}} \\
=& (1+\rho^2)V_1 - a_1V_1^{\frac{\alpha+1}{2}} - b_1V_1^{\frac{1}{2}} \\
=& ((1+\rho^2)V_1^{\frac{1-\alpha}{2}} - \frac{a_1}{2})V_1^{\frac{\alpha+1}{2}} - \frac{a_1}{2}V_1^{\frac{\alpha+1}{2}} - b_1V_1^{\frac{1}{2}},
\end{aligned} \tag{5}$$

where $a_1 = c_1(0)2^{\frac{\alpha+1}{2}}n^{\frac{1-\alpha}{2}}\underline{\lambda}^{\frac{\alpha+1}{2}}$, $b_1 = 2^{\frac{1}{2}}c_2(0)\underline{\lambda}^{\frac{1}{2}}$.

Let $\omega_1 = [\frac{a_1}{2(1+\rho^2)}]^2$, a set $\Omega_1 = \{e(0)|\frac{1}{2}e^T(0)\hat{L}e(0) \leq \omega_1\}$.

Next, we will discuss the following two situations:

Case 1. *If $e(0) \in \Omega_1$, then one has*

$$(1+\rho^2)V^{\frac{1-\alpha}{2}} - \frac{a_1}{2} \leq 0.$$

Therefore, it is easy to know

$$\dot{V}_1 \leq -\frac{a_1}{2}V_1^{\frac{\alpha+1}{2}} - b_1V_1^{\frac{1}{2}}.$$

According to Lemma 2, V_1 converges to zero in a fixed time; that is to say, the system (1) reaches a FXC.

Case 2. *If $e(0) \notin \Omega_1$, that is $V_1(0) > \omega_1$, it can be proved that there exists $T_1 > 0$, satisfying $V_1(t) \leq \omega_1$ for $t \geq T_1$, that is, $e(T_1) \in \{e(T_1)|\frac{1}{2}e^T(T_1)\hat{L}e(T_1) \leq \omega_1\}$. Next, we use reduction to absurdity to verify this situation:*

$$\begin{aligned}
V(T_1) \geq& V(T_1) - V_1(\tau_1) \\
\geq& \int_{\tau_1}^{T_1}((1+\rho^2)V_1 - c_1^*2^{\frac{\alpha+1}{2}}n^{\frac{1-\alpha}{2}}\underline{\lambda}^{\frac{\alpha+1}{2}}V_1^{\frac{\alpha+1}{2}} - 2^{\frac{1}{2}}c_1^*\underline{\lambda}^{\frac{1}{2}}V_1^{\frac{1}{2}})ds \\
>& \int_{T_1}^{\tau_1}(-(1+\rho^2)\omega_1 + c_1^*2^{\frac{\alpha+1}{2}}n^{\frac{1-\alpha}{2}}\underline{\lambda}^{\frac{\alpha+1}{2}}\omega_1^{\frac{\alpha+1}{2}} + 2^{\frac{1}{2}}c_1^*\underline{\lambda}^{\frac{1}{2}}\omega_1^{\frac{1}{2}})ds \\
=& (c_1^*2^{\frac{\alpha+1}{2}}n^{\frac{1-\alpha}{2}}\underline{\lambda}^{\frac{\alpha+1}{2}}\omega_1^{\frac{\alpha+1}{2}} + 2^{\frac{1}{2}}c_1^*\underline{\lambda}^{\frac{1}{2}}\omega_1^{\frac{1}{2}} - (1+\rho^2)\omega_1)(\tau_1 - T_1).
\end{aligned}$$

Since V is bounded, the hypothesis is not tenable when $\tau_1 \to \infty$. So $V_1 \to 0$ in a fixed time.

Combined with the above analysis, V_1 will converge to zero in a fixed time, that is, the system (1) reaches FXC. □

Remark 2. *In [27], Shari and Pourgholi proposed a similar adaptive discontinuous control protocol to study the FXC tracking problem for nonlinear MASs. However, this protocol includes three power state feedbacks with three more complicated adaptive control gain update laws. In comparison, it is natural to find that our control protocol is simpler.*

4. Fixed-Time Leaderless Consensus

In this section, we consider a leaderless MAS consisting of n agents corresponding to the graph G_A, which is also assumed to be detail balanced with positive constants $q_1, q_2, \ldots, q_n$. Its dynamics are

$$\dot{x}_i(t) = f(x_i(t)) + u_i(t), i = 1, 2, \ldots, n, \tag{6}$$

where $x_i(t) \in R^m$ represents the ith agent's state, $f(x_i(t))$ and $u_i(t)$ have the same explanation as in the previous leader-following model (1).

Definition 4. *For system (6), if a positive constant T which is independent of the initial values exists, such that $\lim_{t\to T}(x_i(t) - \frac{1}{n}\sum_{j=1}^{n} x_j(t)) = 0$, and $x_i(t) = \frac{1}{n}\sum_{j=1}^{n} x_j(t), \forall t \geq T$, then the average FXC is reached.*

To drive the system (6) to obtain FXC, we design a discontinuous control protocol for the ith agent as

$$\begin{cases} u_i(t) = c_3(t)\mathrm{sig}^{\alpha}\phi_i(t) + c_4(t)\mathrm{sign}\phi_i(t), \\ \dot{c_3}(t) = \sum_{i=1}^{n} \phi_i(t)\mathrm{sig}^{\alpha}\phi_i(t), \\ \dot{c_4}(t) = \sum_{i=1}^{n} \phi_i(t)\mathrm{sign}\phi_i(t), \end{cases} \tag{7}$$

where $c_3(t), c_4(t)$ are adaptive control strengths with $c_3(0), c_4(0) > 0$, $\alpha > 1$ is the power parameter, and $\phi_i(t) = \sum_{j=1}^{n} q_i a_{ij}(x_j(t) - x_i(t))$.

As in the previous section, in the following part, we also set $m = 1$ and omit the time t. After denoting $x = (x_1, x_2, \ldots, x_n)^T$, $F(x) = (f(x_1), f(x_2), \ldots, f(x_n))^T$, system (6) with the protocol (7) is equivalent to the following matrix form

$$\begin{cases} \dot{x} = F(x) - c_3(t)\mathrm{sig}^{\alpha}(QL_Ax) - c_4(t)\mathrm{sign}(QL_Ax), \\ \dot{c_3}(t) = \|QL_Ax\|_{\alpha+1}^{\alpha+1}, \\ \dot{c_4}(t) = \|QL_Ax\|_1. \end{cases} \tag{8}$$

Next, the conclusion about leaderless MASs is drawn, mainly based on the previous stability theory.

Theorem 2. *Suppose Assumption 1 holds and graph G_A is detail balanced and strongly connected. Then, system (6) will reach average FXC under the given protocol (7).*

Proof. Select a non-negative definite function as

$$\mathbb{V} = \mathbb{V}_1 + \mathbb{V}_2,$$

with $\mathbb{V}_1 = \frac{1}{2}x^T QL_A x$, $\mathbb{V}_2 = \frac{(c_3(t)-c_2^*)^2}{2} + \frac{(c_4(t)-c_2^*)^2}{2}$, where c_2^* is a large enough positive constant.

Additionally, because of the use of discontinuous control protocol, one has the derivative of $\mathbb{V}$ with respect to t as

$$\begin{aligned}\dot{\mathbb{V}} =&\dot{\mathbb{V}}_1 + \dot{\mathbb{V}}_2\\ \in&K[x^T QL_A\dot{x} + (c_3(t) - c_2^*)\dot{c_3}(t) + (c_4(t) - c_2^*)\dot{c_4}(t)]\\ =&x^T QL_A(F(x) - c_3(t)\text{sig}^\alpha(QL_Ax) - c_4(t)\mathbb{S}\text{ign}(QL_Ax))\\ &+ (c_3(t) - c_2^*)||QL_Ax||_{\alpha+1}^{\alpha+1} + (c_4(t) - c_2^*)||QL_Ax||_1.\end{aligned}$$

Again, from the measurable selection theorem [42], we know that there is a measurable function $\mathbb{S}(t) \in \mathbb{S}\text{ign}(QL_Ax)$ that makes the following equation true.

$$\begin{aligned}\dot{\mathbb{V}} =&x^T QL_A(F(x) - c_3(t)\text{sig}^\alpha(QL_Ax) - c_4(t)\mathbb{S}(t))\\ &+ (c_3(t) - c_2^*)||QL_Ax||_{\alpha+1}^{\alpha+1} + (c_4(t) - c_2^*)||QL_Ax||_1\\ =&x^T QL_AF(x) - c_2^*||QL_Ax||_{\alpha+1}^{\alpha+1} - c_2^*||QL_Ax||_1.\end{aligned}$$

Additionally, according to Lemma 1, we can obtain

$$\begin{aligned}x^T QL_AF(x) =&x^T QL_A(F(x) - 1_n \otimes f(\frac{\sum_{i=1}^n x_i}{n}))\\ \leq&\frac{x^T QL_AL_AQ^T x}{2} + \frac{1}{2}(F(x) - 1_n \otimes f(\frac{\sum_{i=1}^n x_i}{n}))^T(F(x) - 1_n \otimes f(\frac{\sum_{i=1}^n x_i}{n}))\\ \leq&\frac{x^T(QL_A)^2x}{2} + \frac{1}{2}\rho\sum_{i=1}^n \|x_i - \frac{\sum_{i=1}^n x_i}{n}\|_2^2\\ =&\frac{x^T(QL_A)^2x}{2} + \frac{1}{2}\rho x^T M^2 x,\end{aligned}$$

where $M = I_n - \frac{1}{n}1_n{1_n}^T$, $MQL_A = QL_AM = QL_A$ and ${1_n}^TM = 0$, I_n is the n-th order identity matrix.

Additionally,

$$\begin{aligned}&x^T(QL_A)^2F(x) \geq \lambda_2(QL_A)x^T QL_Ax,\\ &x^T QL_Ax = x^T MQL_AMx \geq \lambda_2(QL_A)x^T MMx = \lambda_2(QL_A)x^T M^2x.\end{aligned}$$

Then, we have

$$\begin{aligned}x^T QL_AF(x) \leq&\frac{x^T(QL_A)^2x}{2} + \frac{1}{2}\rho\frac{x^T QL_Ax}{\lambda_2(QL_A)}\\ \leq&\frac{x^T(QL_A)^2x}{2} + \frac{1}{2}\rho\frac{x^T(QL_A)^2x}{\lambda_2^2(QL_A)}\\ =&\frac{1}{2}(1 + \frac{\rho}{\lambda_2^2(QL_A)})x^T(QL_A)^2x.\end{aligned}$$

To summarize, by applying inequalities listed in Lemmas 3 and 4, one gets

$$\dot{\mathbb{V}} \leq (1 + \frac{\rho}{\lambda_2^2(QL_A)})x^T(QL_A)^2x - c_2^*n^{\frac{1-\alpha}{2}}(x^T(QL_A)^2x)^{\frac{\alpha+1}{2}} - c_2^*(x^T(QL_A)^2x)^{\frac{1}{2}}. \quad (9)$$

When $c_2^* > 1 + \frac{\rho}{\lambda_2^2(QL_A)}$, one has that

$$\dot{\mathbb{V}} \leq 0.$$

This shows that $\mathbb{V}$ is bounded.
From (9), one has

$$\begin{aligned}
\dot{\mathbb{V}}_1 =&\dot{\mathbb{V}} - \dot{\mathbb{V}}_2 \\
\leq& x^T QL_A F(x) - c_2^* ||QL_A x||_{\alpha+1}^{\alpha+1} - c_2^* ||QL_A x||_1 - (c_3(t) - c_2^*)||QL_A x||_{\alpha+1}^{\alpha+1} \\
&- (c_4(t) - c_2^*)||QL_A x||_1 \\
=& x^T QL_A F(x) - c_3(t)||QL_A x||_{\alpha+1}^{\alpha+1} - c_4(t)||QL_A x||_1 \\
\leq& x^T QL_A F(x) - c_3(0)||QL_A x||_{\alpha+1}^{\alpha+1} \\
&- c_4(0)||QL_A x||_1 \\
\leq& \frac{1}{2}(1 + \frac{\rho}{\lambda_2^2(L_A)})x^T (QL_A)^2 x - c_3(0) n^{\frac{1-\alpha}{2}} (x^T (QL_A)^2 x)^{\frac{\alpha+1}{2}} \\
&- c_4(0)(x^T (QL_A)^2 x)^{\frac{1}{2}} \\
=& \frac{1}{2}(1 + \frac{\rho}{\lambda_2^2(L_A)})x^T (QL_A)^2 x - a_2 (x^T (QL_A)^2 x)^{\frac{\alpha+1}{2}} - b_2 (x^T (QL_A)^2 x)^{\frac{1}{2}} \\
=& (\frac{1}{2}(1 + \frac{\rho}{\lambda_2^2(L_A)})(x^T (QL_A)^2 x)^{\frac{1-\alpha}{2}} - \frac{a_2}{2})(x^T (QL_A)^2 x)^{\frac{\alpha+1}{2}} \\
&- \frac{a_2}{2}(x^T (QL_A)^2 x)^{\frac{\alpha+1}{2}} - b_2 (x^T (QL_A)^2 x)^{\frac{1}{2}},
\end{aligned} \tag{10}$$

where $a_2 = c_3(0) n^{\frac{1-\alpha}{2}}, b_2 = c_4(0)$.

Let $\omega_2 = [\frac{a_2 \lambda_2^2(L_A)}{\lambda_2^2(L_A)+\rho}]^{\frac{2}{1-\alpha}}$, and $\Omega_2 = \{x(0) | \frac{1}{2} x^T(0)(QL_A)^2 x(0) \leq \omega_2\}$.

Next, we will discuss the following two situations:

Case 1. *If $x(0) \in \Omega_2$, then one has*

$$\frac{1}{2}(1 + \frac{\rho}{\lambda_2^2(L_A)})(x^T (QL_A)^2 x)^{\frac{1-\alpha}{2}} - \frac{a_2}{2} \leq 0.$$

Therefore, it is easy to know

$$\begin{aligned}
\dot{\mathbb{V}}_1 \leq& -\frac{a_2}{2}(x^T (QL_A)^2 x)^{\frac{\alpha+1}{2}} - b_2 (x^T (QL_A)^2 x)^{\frac{1}{2}} \\
\leq& -\frac{a_2}{2}(\lambda_2(L_A) x^T QL_A x)^{\frac{\alpha+1}{2}} - b_2 (\lambda_2(L_A) x^T QL_A x)^{\frac{1}{2}} \\
=& -a_2 2^{\frac{\alpha-1}{2}} \lambda_2^{\frac{\alpha+1}{2}}(L_A) \mathbb{V}_1^{\frac{\alpha+1}{2}} - b_2 2^{\frac{1}{2}} \lambda_2^{\frac{1}{2}}(L_A) \mathbb{V}_1^{\frac{1}{2}}.
\end{aligned}$$

According to Lemma 2, we get $\mathbb{V}_1$ converges to zero in a fixed time; that is to say, the system (6) reaches FXC.

Case 2. *If $x(0) \notin \Omega_2$, that is $\mathbb{V}_1(0) > \omega_2$, it can be proven that there exists $T_2 > 0$ satisfying $\mathbb{V}_1(t) \leq \omega_2$ for $t \geq T_2$; that is, $x(T_2) \in \{x(T_2) | \frac{1}{2} x^T(T_2)(QL_A)^2 x(T_2) \leq \omega_2\}$. Next, we use reduction to absurdity to verify this situation:*

$$\begin{aligned}
\mathbb{V}(T_2) \geq& \mathbb{V}(T_2) - \mathbb{V}_1(\tau_2) \\
\geq& \int_{\tau_2}^{T_2} (1 + \frac{\rho}{\lambda_2^2(QL_A)})x^T (QL_A)^2 x - c_2^* n^{\frac{1-\alpha}{2}} (x^T (QL_A)^2 x)^{\frac{\alpha+1}{2}} - c_2^* (x^T (QL_A)^2 x)^{\frac{1}{2}} ds \\
>& \int_{T_2}^{\tau_2} -(1 + \frac{\rho}{\lambda_2^2(QL_A)})\omega_2 + c_2^* n^{\frac{1-\alpha}{2}} (\omega_2)^{\frac{\alpha+1}{2}} + c_2^* (\omega_2)^{\frac{1}{2}} ds \\
=& (-(1 + \frac{\rho}{\lambda_2^2(QL_A)})\omega_2 + c_2^* n^{\frac{1-\alpha}{2}} (\omega_2)^{\frac{\alpha+1}{2}} + c_2^* (\omega_2)^{\frac{1}{2}})(\tau_2 - T_2).
\end{aligned}$$

Since $\mathbb{V}$ is bounded, the hypothesis is not tenable when $\tau_2 \to \infty$. So $\mathbb{V}_1 \to 0$ in a fixed time.

Combined with the above analysis, $\mathbb{V}_1$ will converge to zero in a fixed time; that is, the system (6) reaches FXC. □

Remark 3. *Two protocols are used to consider the FXC for nonlinear MASs in above two sections. They are relatively simple compared to other studies on the same topic [1,27,32–37], because they only contain two terms. One is the sign information of the state error between one agent and its neighbors, and the other is the state feedback with power greater than one.*

Remark 4. *In [1,27], the authors studied the FXC problem of MASs with node-based and edge-based adaptive control protocols, respectively. It can be seen from the control protocols provided that each agent or each edge in the system will correspond to at least an adaptive updating law. In other words, if the system scale is large, the dimension of the system model will be dramatically increased under such control protocols, which will increase the computational complexity and control cost. However, in our proposed control protocol, only two adaptive updating laws are needed without considering the scale of the system.*

Remark 5. *When control protocols (2) and (7) are applied to real networks, some sensors are needed to obtain the state error between each agent and its neighbors. Then, the state errors of all agents and their neighbors should be integrated, and the time-varying control gains $c_i(t)$ are determined according to the adaptive updating laws. Finally, the protocols $u_i(t)$ proposed in this paper are used to control the considered system to ensure the FXC.*

Remark 6. *Generally, controllers with signum function are widely used in the cooperative control for MASs because they not only can improve the convergence rate of system but also can be realized by some simple electronic circuits [43]. However, the chattering phenomenon caused by signum function is hard to avoid. Therefore, some scholars began to design the controllers without signum function to overcome the chattering phenomenon. For example, a quantized pinning synchronization controller without signum function was proposed in [44] to avoid the chattering phenomenon; in [45], some saturation functions were constructed to replace the sign function to suppress the chattering.*

5. Illustrative Example

The multi-agent-based supply chain network is a dynamic system consisting of multiple subchains that exchange information and materials between enterprises, as shown in Figure 1.

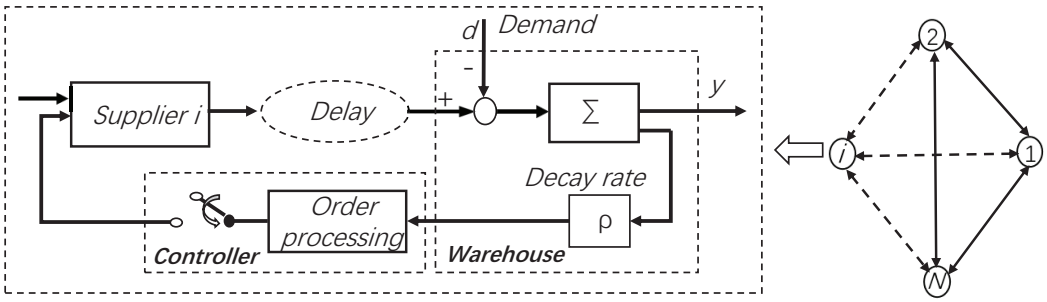


Figure 1. Multi-agent-based supply chain network with N sub-chains.

In [46], a chaotic three-echelon supply chain is presented, whose dynamics are shown as

$$\begin{cases} \dot{x}_1(t) = mx_2(t) - (n+1)x_1(t), \\ \dot{x}_2(t) = rx_1(t) - x_2(t) - x_1(t)x_3(t), \\ \dot{x}_3(t) = x_1(t)x_2(t) + (k-1)x_3(t), \end{cases}$$

where $x_1(t), x_2(t), x_3(t)$ stand for the number of retailers required in this period, the amount of products that distributors can deliver, and the quantity produced depending on the order, respectively. m represents the retailer's customer demand satisfaction rate. n denotes

the level of distributors' inventory. k is manufacturer's safety stock factor. r indicates the rate of product information distortion. The nonlinear supply chain network exhibits chaotic behavior when $m = 12, n = 7, r = 45, k = -\frac{7}{3}$ [46]. We set the multi-agent based three-echelon supply chain network that was given in [6] as our example to verify the validity of the proposed control protocols.

5.1. Fixed-Time Leader-Following Consensus Example

This subsection takes an example consisting of a single leader and five followers in three-dimensional space as an example to verify the correctness of the proposed Theorem 1. To make the leader become the root node of the example topology graph, the weighted adjacency matrix A and the leader adjacency matrix A_0 of the example are given as

$$A = \begin{pmatrix} 0 & 2 & 2 & 0 & 0 \\ 3 & 0 & 3 & 0 & 0 \\ 3 & 3 & 0 & 0 & 0 \\ 0 & 0 & 0 & 0 & 4 \\ 0 & 0 & 0 & 1 & 0 \end{pmatrix}, A_0 = \begin{pmatrix} 2 & 0 & 0 & 0 & 0 \\ 0 & 1 & 0 & 0 & 0 \\ 0 & 0 & 0 & 0 & 0 \\ 0 & 0 & 0 & 2 & 0 \\ 0 & 0 & 0 & 0 & 0 \end{pmatrix}.$$

The topology graph of the leader-following multi-agent-based three-echelon supply chain network is given in Figure 2. Obviously, the weighted adjacency matrix A is detail balanced with $q_1 = \frac{1}{2}, q_2 = \frac{1}{3}, q_3 = \frac{1}{3}, q_4 = \frac{1}{4}, q_5 = 1$.

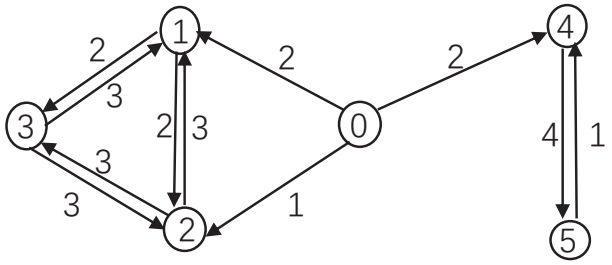


Figure 2. Communication topology of a leader-following multi-agent-based supply chain network.

To demonstrate the influence of different initial states on FXC, we give the following initial values: (1): $x_1(0) = (-1, 2, 3)^T, x_2(0) = (4, -2, 1)^T, x_3(0) = (-3, 1, 2)^T$, $x_4(0) = (-1, 3, -1)^T, x_5(0) = (2, 4, -2)^T, x_0(0) = (1, 2, 1)^T$; (2): $x_1(0) = (-5, 10, 15)^T$, $x_2(0) = (20, -10, 5)^T, x_3(0) = (-15, 5, 10)^T, x_4(0) = (-5, 15, -5)^T, x_5(0) = (10, 20, -10)^T$, $x_0(0) = (5, 10, 5)^T$. The external disturbance is chosen as $d_i(t) = 1 + sin(cos(\frac{\pi}{2}t))$.

We set $\alpha = 1.2$ to verify the validity of the control protocol (2) in facilitating the example to obtain FXC. Figures 3–5 show that all followers can catch up with the leader after a transient of about 0.3s under initial values (1) and (2). Figure 6 shows the control curve of the adaptive law $c_1(t)$ and $c_2(t)$. These two figures also imply that when the initial values differ greatly, the change in convergence time is not very obvious, which verifies the advantage of the FXC. Therefore, the simulation results effectively verify the validity of the theoretical analysis in Theorem 1.

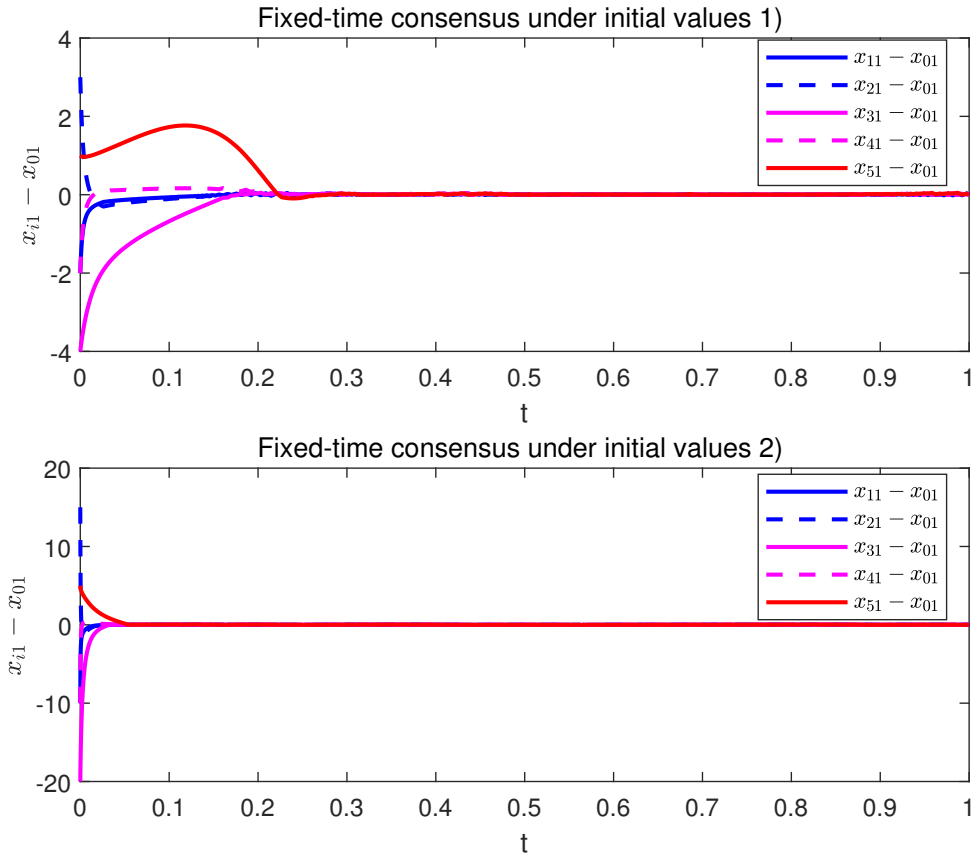


Figure 3. The trajectories of x_{i1} for leader-following example under initial values (1) and (2).

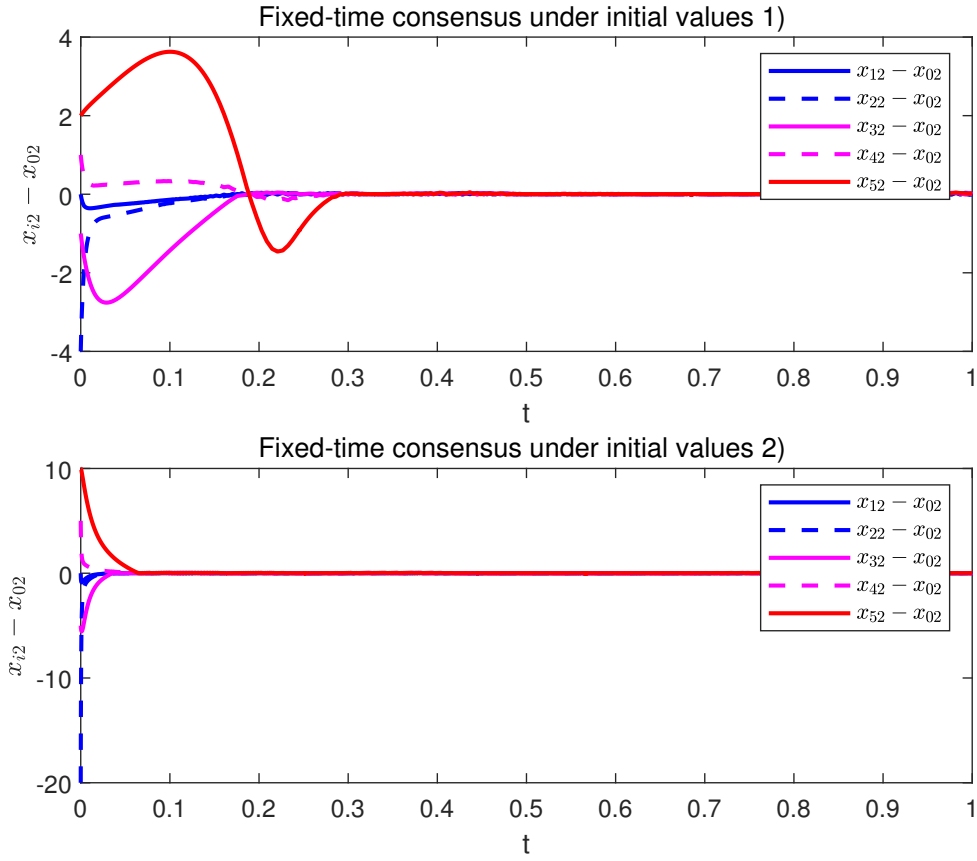


Figure 4. The trajectories of x_{i2} for leader-following example under initial values (1) and (2).

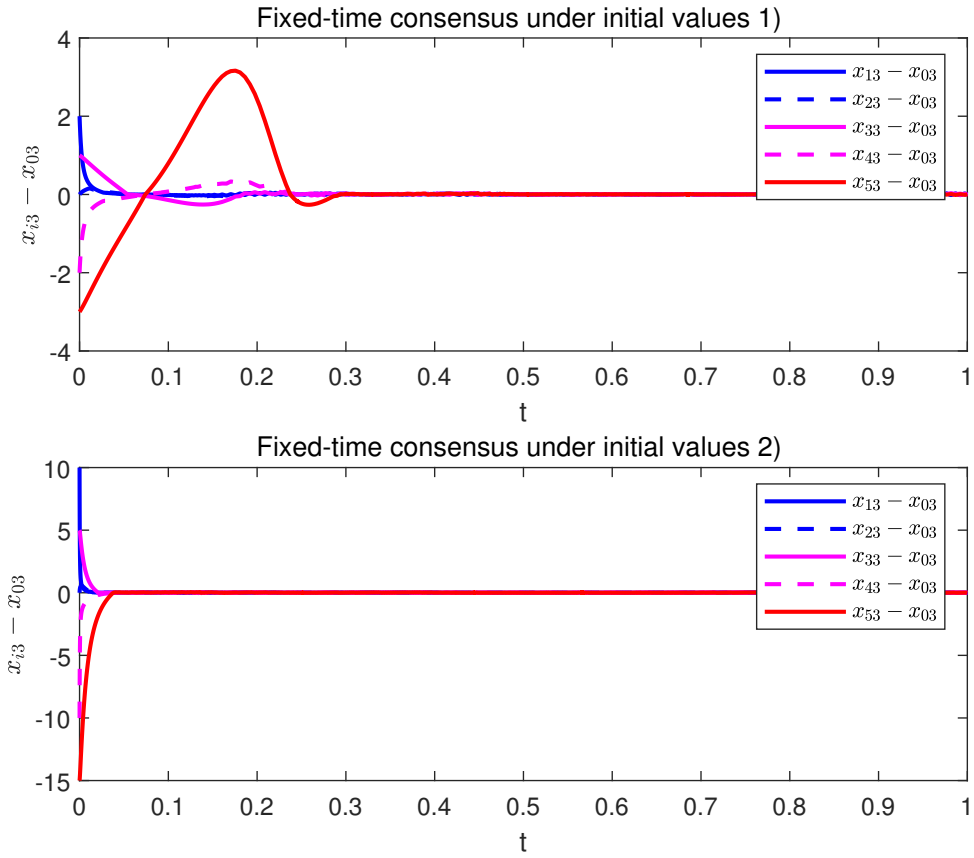


Figure 5. The trajectories of x_{i3} for leader-following example under initial values (1) and (2).

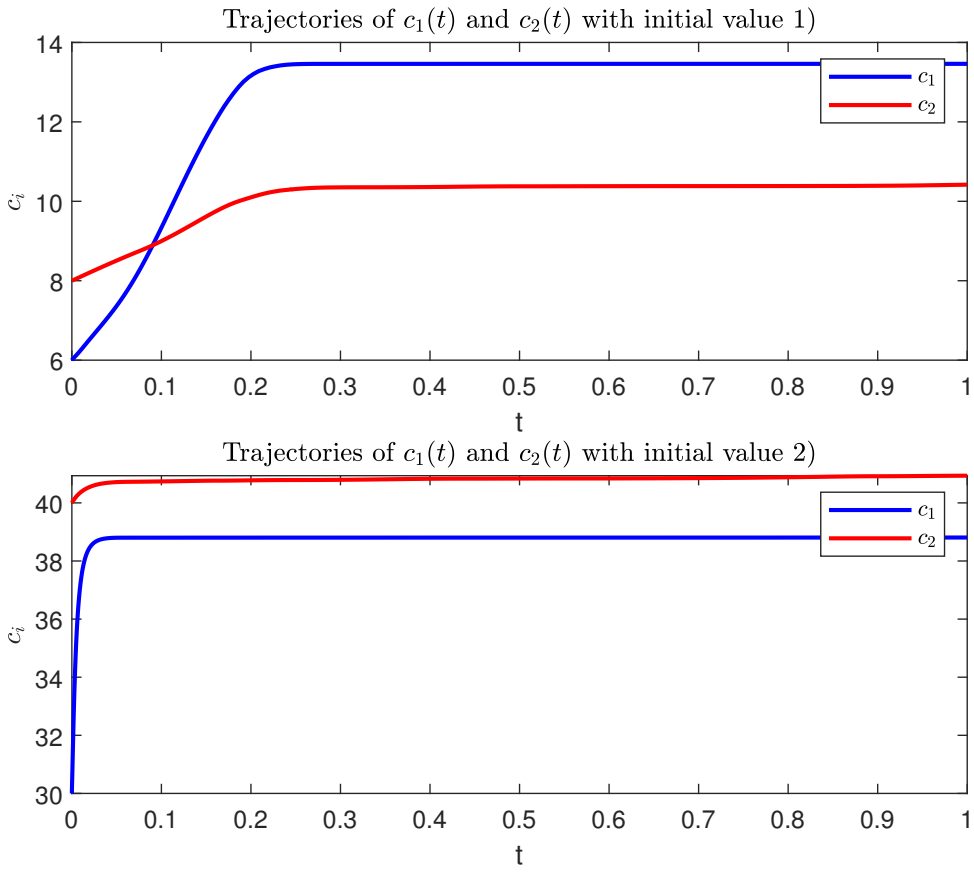


Figure 6. The trajectories of $c_1(t)$ and $c_2(t)$ under initial values (1) and (2).

5.2. Fixed-Time Leaderless Consensus Example

This subsection considers a leaderless MAS of five agents in three-dimensional space as an example to illustrate the effectiveness of Theorem 2. Figure 7 indicates the interaction of five three-echelon supply subchains. The weighted adjacency matrix A is given as

$$A = \begin{pmatrix} 0 & 2 & 2 & 0 & 0 \\ 1 & 0 & 0.5 & 0 & 0 \\ 1 & 0.5 & 0 & 1 & 0 \\ 0 & 0 & 1 & 0 & 1 \\ 0 & 0 & 0 & 1 & 0 \end{pmatrix}.$$

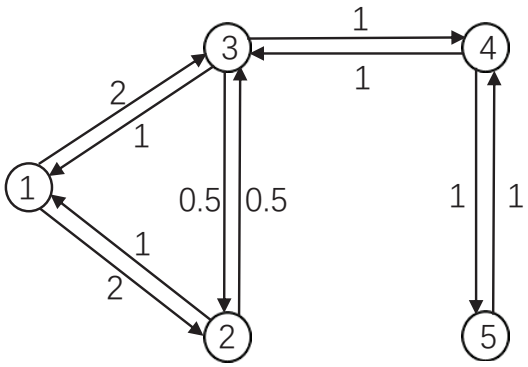


Figure 7. Communication topology of leaderless multi-agent based supply chain network.

It is easy to see from the adjacency matrix A that its corresponding topology graph is strongly connected. The weighted adjacency matrix A is detail balanced with $q_1 = 0.5$, $q_2 = q_3 = q_4 = q_5 = 1$.

Similarly, we take two very different sets of initial values: (1): $x_1(0) = (-1, 2, 3)^T$, $x_2(0) = (4, -2, 1)^T, x_3(0) = (-3, 1, 2)^T, x_4(0) = (-1, 3, -1)^T, x_5(0) = (2, 4, -2)^T$; 2): $x_1(0) = (-5, 10, 15)^T$, $x_2(0) = (20, -10, 5)^T, x_3(0) = (-15, 5, 10)^T$, $x_4(0) = (-5, 15, -5)^T$, $x_5(0) = (10, 20, -10)^T$, $x_0(0) = (5, 10, 5)^T$ to reveal changes in convergence time. The nonlinear function $f(x)$ is the same as the case of above leader-following example.

Here, we also select $\alpha = 1.2$ to demonstrate the availability of our control protocol (8) on the average FXC of this leadless example. Figures 8–10 tell us that under two different initial values, all agents can reach consensus in about 0.4s. Additionally, the settling time does not change significantly with the great change in the initial values. The curves of the adaptive control laws are shown in Figure 11.

In contrast with the existing literature [12–15,17,19–21], a strange thing seems to happen in the above two simulation examples; that is, the larger the initial value of the system, the shorter the convergence time. The reason is that the larger the initial values of the system, the faster the control gains increase. In a very short time, they can reach a large value, thus shortening the convergence time of the system.

Compared with [9,10], the numerical simulation here shows that under the control protocol we give, the system can achieve consensus in a very short time, which indicates that the convergence speed of fixed-time consensus is very fast. Moreover, compared with [21–24], in our simulation process, the eigenvalues of the Laplacian matrix and parameters of the control protocol do not need to be calculated, and the Lipschtiz constant of nonlinear dynamic properties does not need to be considered.

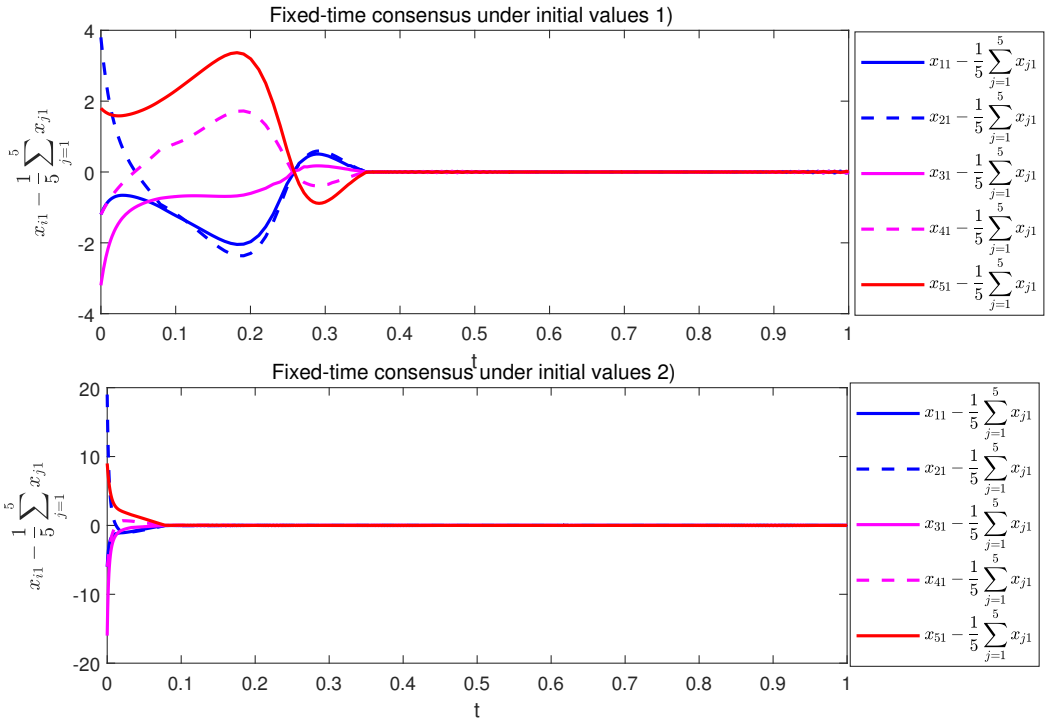


Figure 8. The trajectories of x_{i1} for leaderless example under initial values (1) and (2).

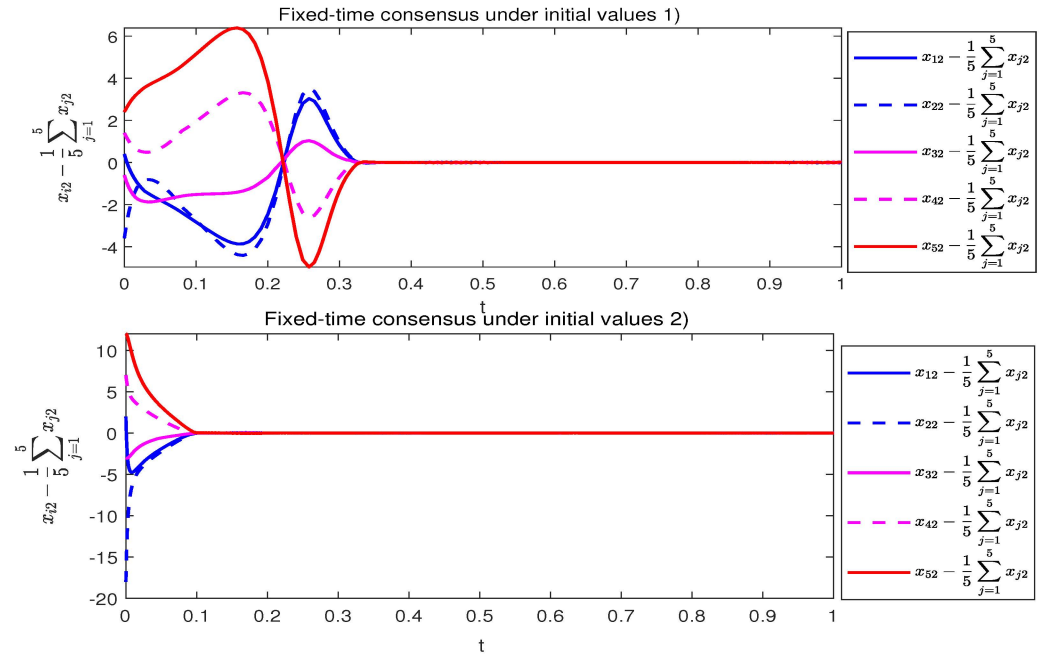


Figure 9. The trajectories of x_{i2} for leaderless example under initial values (1) and (2).

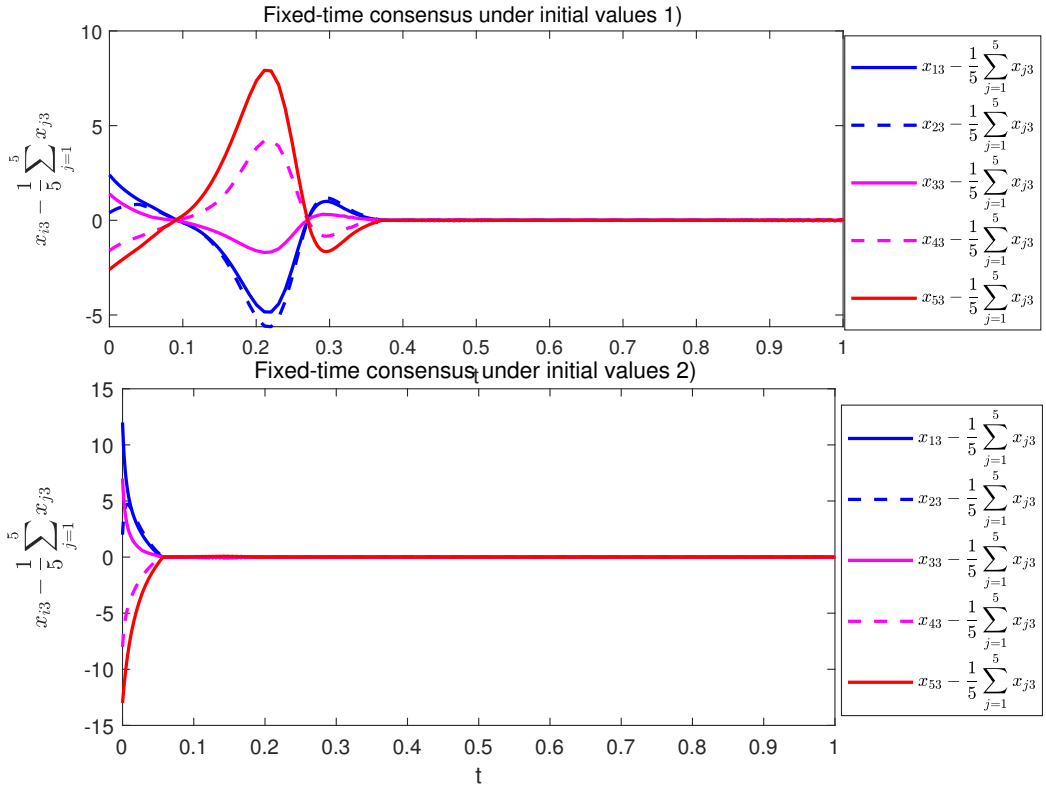


Figure 10. The trajectories of x_{i3} for leaderless example under initial values (1) and (2).

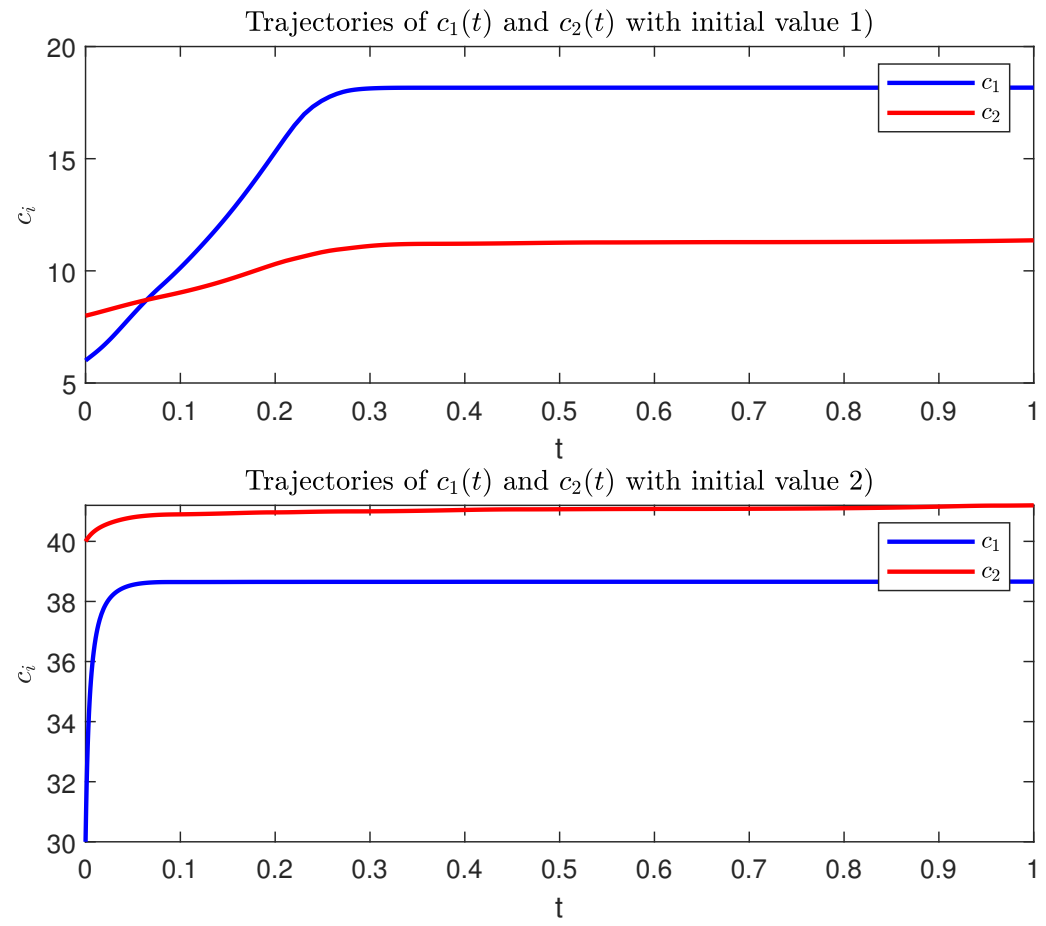


Figure 11. The curves of $c_1(t)$ and $c_2(t)$ with different initial values (1) and (2).

6. Conclusions

In this paper, we study the FXC control problem for nonlinear leader-following and leaderless MASs on a detailed-balance graph. Two simple adaptive discontinuous control protocols are proposed to drive our considered systems to FXC. Structurally, the proposed control protocols only need the state measurement error and its sign information. Furthermore, the protocols presented here require very few adaptive update laws and are much simpler than the common node-based and edge-based adaptive protocols. As mentioned above, the control protocol presented in this paper needs to know the adjacency matrix of the system in advance, and the chattering issues may occur during the control process. These shortcomings will motivate us to design even more superior algorithms in our future work.

Author Contributions: Conceptualization, L.W., M.Z., W.G., H.A., A.A., R.O.A.T. and H.J.; methodology, L.W., M.Z., W.G., H.A., A.A., R.O.A.T. and H.J.; software, L.W., M.Z., W.G., H.A., A.A., R.O.A.T. and H.J.; validation, L.W., M.Z., W.G., H.A., A.A., R.O.A.T. and H.J.; investigation, L.W., M.Z., W.G., H.A., A.A., R.O.A.T. and H.J.; writing—original draft preparation, L.W., M.Z., W.G., H.A., A.A., R.O.A.T. and H.J.; writing—review and editing, L.W., M.Z., W.G., H.A., A.A., R.O.A.T. and H.J.; supervision, L.W., M.Z., W.G., H.A., A.A., R.O.A.T. and H.J. All authors have read and agreed to the published version of the manuscript.

Funding: This work is supported in part from the National Natural Science Foundation of China (12071446).

Data Availability Statement: Data available on request from the authors.

Conflicts of Interest: The authors declare no conflict of interest.

References

1. Cao, Y.; Yu, W.; Ren, W.; Chen, G. An overview of recent progress in the study of distributed multi-agent coordination. *IEEE Trans. Ind. Inform.* **2013**, *9*, 427–438. [CrossRef]
2. Wang, X.; Hong, Y.; Ji, H. Distributed optimization for a class of nonlinear multiagent systems with disturbance rejection. *IEEE Trans. Cybern.* **2016**, *46*, 1655–1666. [CrossRef] [PubMed]
3. Li, D.; Ge, S.S.; He, W.; Ma, G.; Xie, L. Multilayer formation control of multi-agent systems. *Automatica* **2019**, *109*, 108558. [CrossRef]
4. Dong, R.; Geng, Z. Consensus for formation control of multi-agent systems. *Int. J. Robust Nonlinear Control* **2015**, *25*, 2481–2501. [CrossRef]
5. Li, Q.; Lin, H.; Tan, X.; Du, S. H^{∞} consensus for multiagent-based supply chain systems under switching topology and uncertain demands. *IEEE Trans. Syst. Man, Cybern. Syst.* **2020**, *50*, 4905–4918. [CrossRef]
6. Liu, Z.; Jahanshahi, H.; Volos, C.; Bekiros, S.; He, S.; Alassafi, M.O.; Ahmad, M. Distributed consensus tracking control of chaotic multi-agent supply chain network: A new fault-tolerant, finite-time, and chatter-free approach. *Entropy* **2022**, *24*, 33. [CrossRef]
7. Wang, P.; Wang, D.; Lv, J. Controllability analysis of a gene network for arabidopsis thaliana reveals characteristics of functional gene families. *IEEE-ACM Trans. Comput. Biol. Bioinform.* **2019**, *16*, 912–924. [CrossRef]
8. Dorfler, F.; Bullo, F. Synchronization and transient stability in power networks and nonuniform kuramoto oscillators. *SIAM J. Control Optim.* **2012**, *50*, 1616–1642. [CrossRef]
9. Yang, J.; Feckan, M.; Wang, J. Consensus problems of linear multi-agent systems involving conformable derivative. *Appl. Math. Comput.* **2021**, *394*, 125809. [CrossRef]
10. Tan, C.; Dong, X.; Li, Y.; Liu, G. Leader-following consensus problem of networked multi-agent systems under switching topologies and communication constraints. *IET Control Theory Appl.* **2020**, *14*, 3686–3696. [CrossRef]
11. Kim, J.; Yang, J.; Shim, H.; Kim, J.; Seo, J. Robustness of synchronization of heterogeneous agents by strong coupling and a large number of agents. *IEEE Trans. Autom. Control* **2015**, *61*, 3096–3102. [CrossRef]
12. Tian, X.; Liu, H.; Liu, H. Robust finite-time consensus control for multi-agent systems with disturbances and unknown velocities. *ISA Trans.* **2018**, *80*, 73–80. [CrossRef] [PubMed]
13. Wang, Y.; Yuan, Y.; Liu, J. Finite-time leader-following output consensus for multi-agent systems via extended state observer. *Automatica* **2021**, *124*, 109133. [CrossRef]
14. Lu, J.; Wang, Y.; Shi, X.; Cao, J. Finite-time bipartite consensus for multiagent systems under detail-balanced antagonistic interactions. *IEEE Trans. Syst. Man, Cybern. Syst.* **2021**, *51*, 3867–3875. [CrossRef]
15. Zhao, Y.; Liu, Y.; Wen, G.; Ren, W.; Chen, G. Edge-based finite-time protocol analysis with final consensus value and settling time estimations. *IEEE Trans. Cybern.* **2020**, *50*, 1450–1459. [CrossRef]

16. Zuo, Z.; Tie, L. A new class of finite-time nonlinear consensus protocols for multi-agent systems. *Int. J. Control* **2014**, *87*, 363–370. [CrossRef]
17. Ning, B.; Han, Q.; Zuo, Z. Practical fixed-time consensus for integrator-type multi-agent systems: A time base generator approach. *Automatica* **2019**, *105*, 406–414. [CrossRef]
18. Ai, X.; Wang, L. Distributed fixed-time event-triggered consensus of linear multi-agent systems with input delay. *Int. J. Robust Nonlinear Control* **2021**, *31*, 2526–2545. [CrossRef]
19. Chen, T.; Shan, J. Fixed-time consensus control of multiagent systems using input shaping. *IEEE Trans. Ind. Electron.* **2019**, *66*, 7433–7440. [CrossRef]
20. Ni, J.; Tang, Y.; Shi, P. A new fixed-time consensus tracking approach for second-order multiagent systems under directed communication topology. *IEEE Trans. Syst. Man, Cybern. Syst.* **2021**, *51*, 2488–2500. [CrossRef]
21. Liu, J.; Yu, Y.; Wang, Q.; Sun, C. Fixed-time event-triggered consensus control for multi-agent systems with nonlinear uncertainties. *Neurocomputing* **2017**, *260*, 497–504. [CrossRef]
22. Dong, Y.; Chen, J.; Cao, J. Fixed-time consensus of nonlinear multi-agent systems with stochastically switching topologies. *Int. J. Control* **2022**, *95*, 2828–2839. [CrossRef]
23. Xu, Z.; Liu, X.; Cao, J.; Song, M. Fixed-time bipartite consensus of nonlinear multi-agent systems under directed signed graphs with disturbances. *J. Frankl. Inst.* **2022**, *359*, 2693–2709. [CrossRef]
24. Wang, C.; Liu, C.; Chen, Y.; Zhang, Y. Fixed-time consensus tracking for second-order leader-follower multi-agent systems with nonlinear dynamics under directed topology. *Int. J. Control Autom. Syst.* **2021**, *19*, 2697–2705. [CrossRef]
25. Cai, Y.; Zhang, H.; Zhang, J.; Wang, W. Fixed-time leader-following/containment consensus for a class of nonlinear multi-agent systems. *Inf. Sci.* **2021**, *555*, 58–84. [CrossRef]
26. Ni, J.; Shi, P. Adaptive neural network fixed-time leader-follower consensus for multiagent systems with constraints and disturbances. *IEEE Trans. Cybern.* **2021**, *51*, 1835–1848. [CrossRef]
27. Sharifi, A.; Pourgholi, M. Adaptive controller design for fixed-time leader-following consensus of multi-agent systems with discontinuous dynamics. *Int. J. Control* **2022**, *95*, 830–839. [CrossRef]
28. Liu, S.; Wang, H.; Li, T.; Xu, K. Adaptive Neural Fixed-time Control for Uncertain Nonlinear Systems. *IEEE Trans. Circuits Syst. II Express Briefs* **2022**, *early access*.[CrossRef]
29. Mei, Y.; Wang, J.; Park, J.; Shi, K. Adaptive fixed-time control for nonlinear systems against time-varying actuator faults. *Nonlinear Dyn.* **2022**, *107*, 3629–3640. [CrossRef]
30. Du, Z.; Liang, H.; Xue, H. Fixed-time adaptive anti-disturbance and fault-tolerant control for multi-agent systems. *Int. J. Robust Nonlinear Control* **2022**, *32*, 6684–6703. [CrossRef]
31. Bai, W.; Liu, X.; Wang, H. Adaptive fixed-time fuzzy control for nonlinear systemswith actuator faults. *Int. J. Adapt. Control Signal Process.* **2022**, *36*, 762–784. [CrossRef]
32. Liu, X.; Ho, D.W.C.; Song, Q.; Xu, W. Finite/Fixed-Time pinning synchronization of complex networks with stochastic disturbances. *IEEE Trans. Cybern.* **2019**, *49*, 2398–2403. [CrossRef]
33. Ning, B.; Zuo, Z.; Jin, J.; Zheng, J. Distributed fixed-time coordinated tracking for nonlinear multi-agent systems under directed graphs. *Asian J. Control* **2018**, *20*, 646–658. [CrossRef]
34. Ji, G.; Hu, C.; Yu, J.; Jiang, H. Finite-time and fixed-time synchronization of discontinuous complex networks: A unified control framework design. *J. Frankl. Inst.* **2018**, *355*, 4665–4685. [CrossRef]
35. Liu, X.; Ho, D.; Cao, J.; Xu, W. Discontinuous observers design for finite-time consensus of multiagent systems with external disturbances. *IEEE Trans. Neural Netw. Learn. Syst.* **2017**, *28*, 2826–2830. [CrossRef]
36. Ning, B.; Jin, J.; Zheng, J.; Man, Z. Finite-time and fixed-time leader-following consensus for multi-agent systems with discontinuous inherent dynamics. *Int. J. Control* **2018**, *91*, 1259–1270. [CrossRef]
37. Sader, M.; Chen, Z.; Liu, Z.; Deng, C. Distributed robust fault-tolerant consensus control for a class of nonlinear multi-agent systems with intermittent communications. *Appl. Math. Comput.* **2021**, *403*, 126166. [CrossRef]
38. Olfati-Saber, R.; Murray, R.M. Consensus problems in networks of agents with switching topology and time-delays. *IEEE Trans. Autom. Control* **2004**, *49*, 1520–1533. [CrossRef]
39. Hardy, G.; Littlewood, J.E.; Pólya, G. *Inequalities*; Cambridge University Press: Cambridge, UK, 1988.
40. Lu, W.; Liu, X.; Chen, T. A note on finite-time and fixed-time stability. *Neural Netw. Lett.* **2016**, *81*, 11–15. [CrossRef]
41. Tao, T.; Roy, S.; Baldi, S. Adaptive synchronization of uncertain complex networks under state-dependent a priori interconnections. In Proceedings of the 60th IEEE Conference on Decision and Control, Austin, TX, USA, 14–17 December 2021; pp. 1777–1782.
42. Filippov, A.F.; Arscott, F.M. *Differential Equations with Discontinous Righthand Sides*; Springer: Berlin/Heidelberg, Germany, 1988.
43. Chen, G.; Lewis, F.L.; Xie, L. Finite-time distributed consensus via binary control protocols. *Automatica* **2011**, *47*, 1962–1968. [CrossRef]
44. Zhang, W.; Li, H.; Li, C.; Li, Z.; Yang, X. Fixed-time synchronization criteria for complex networks via quantized pinning control. *ISA Trans.* **2019**, *91*, 151–156. [CrossRef] [PubMed]
45. Hu, C.; Jiang, H. Special functions-based fixed-time estimation and stabilization for dynamic systems. *IEEE Trans. Syst. Man Cybern. Syst.* **2022**, *52*, 3251–3262. [CrossRef]
46. Anne, K.R.; Chedjou, J.C.; Kyamakya, K. Bifurcation analysis and synchronisation issues in a three-echelon supply chain. *Int. J.-Logist.-Res. Appl.* **2009**, *12*, 347–362. [CrossRef]